Science Bulletin 64 (2019) 1418–1425

Contents lists available at ScienceDirect

Science Bulletin

journal homepage: www.elsevier.com/locate/scib

Article

Biomimetic intestinal barrier based on microfluidic encapsulated sucralfate microcapsules

Cheng Zhao [a], Yunru Yu [b], Xiaoxuan Zhang [b], Xiuwen Wu [a], Jianan Ren [a,*], Yuanjin Zhao [a,b,*]

[a] Department of General Surgery, Jinling Hospital, Medical School of Nanjing University, Nanjing 210002, China
[b] State Key Laboratory of Bioelectronics, School of Biological Science and Medical Engineering, Southeast University, Nanjing 210096, China

ARTICLE INFO

Article history:
Received 25 April 2019
Received in revised form 26 May 2019
Accepted 11 July 2019
Available online 19 July 2019

Keywords:
Biomimetic
Microfluidics
Microcapsule
Intestinal barrier
Gastrointestinal disease

ABSTRACT

Intestinal barriers play an important role in preventing intestinally derived diseases, and maintaining their function is a promising approach to prevent and treat those diseases. Here, inspired by the protection effect of intestinal barriers in live organisms and the mucosa adhesive property of sucralfate, we present a biomimetic intestinal barrier based on microfluidic encapsulated sucralfate microcapsules. Benefiting from the flexible selectivity and precise control of microfluidic electrospray flows, the generated microcapsules were imparted with stomach-tolerant dietary-fibre shells and controllable released sucralfate cores, both of which could contribute to forming a continuous biomimetic intestinal barrier on the intestine. Through in vitro adhesive study, in vivo computed tomography (CT) imaging and in vivo imaging system (IVIS) methods, we have demonstrated that the microcapsule-derived biomimetic intestinal barrier can effectively block food fermentation in the gut, reduce generation of fat, decrease disease risk indexes, and prevent obesity. These features make the microfluidic encapsulated sucralfate microcapsules and their resultant biomimetic intestinal barrier an approach for treating obesity and other intestinal diseases.

1. Introduction

An intestinal barrier is the gap between mixing of luminal antigenic material and internal milieu, and it controls nutrient absorption and prevents pathogen invasions [1–3]. As it is exposed to many dangerous factors, including increased energy consumption, drug abuse and environment pollution, the intestinal barrier usually faces the risk of aberration, which may lead to many diseases, such as diabetes, obesity, and organ failure [2]. So far, numerous methods including chemical drugs, bioactive adhesives and health products, have been explored to cure these diseases by removing inner pathogens, correcting microbiota dysbiosis, or restoring barrier function [4–10]. Among these methods, bioactive mucosal adhesives, such as sucralfate and its derivatives that can form a protective gel in the stomach, are the most attractive candidates due to their ability to adhere on wet tissue, accelerate ulcer healing, prevent bleeding, inhibit acid invasion, and partially restore barrier function [11–13]. However, the gelling process in the stomach usually causes loss of efficient actives making it unstable in the digestive tract and unable to disperse continuously on the intestine. Additionally, owing to the complex environment in the intestine, the residual stomach sucralfate degraded quickly and was not stable on the mucosa with digestive fluid disturbance. As a result, sucralfate cannot work efficiently in the small intestine and their value in the intestine is limited. Thus, the creation of a novel biomimetic mucosal adhesive system that can work efficiently on the whole small intestine is still anticipated.

In this paper, we proposed a biomimetic intestinal barrier based on microfluidic encapsulated sucralfate microcapsules for intestinal protection and pathogen blocking that lines the whole gut and protects the body from luminal pathogens, as shown in Fig. 1. Benefiting from their capability to separate liquid cargo and solid encapsulant as well as high cargo content, microcapsules have been widely applied in encapsulation, delivery, and release of actives in the fields of agriculture, cosmetics, drug delivery, detergents, and food additives [14–18]. A variety of techniques, such as spray drying, interfacial polymerization, complex coacervation, and microfluidics, have been employed for the preparation of functional microcapsules [19–26]. Among these methods, the microfluidics technologies can overcome limitations associated with variability during microcapsule production and generate functional microcapsules with fine-tuned chemical compositions, shell thicknesses, and encapsulant volume ratios by the precise control of their multiphasic flow [15–17,27–32]. However, encapsulating highly viscous materials in microfluidic microcapsules presents

* Corresponding authors.
E-mail addresses: jiananr@gmail.com (J. Ren), yjzhao@seu.edu.cn (Y. Zhao).

https://doi.org/10.1016/j.scib.2019.07.020
2095-9273/

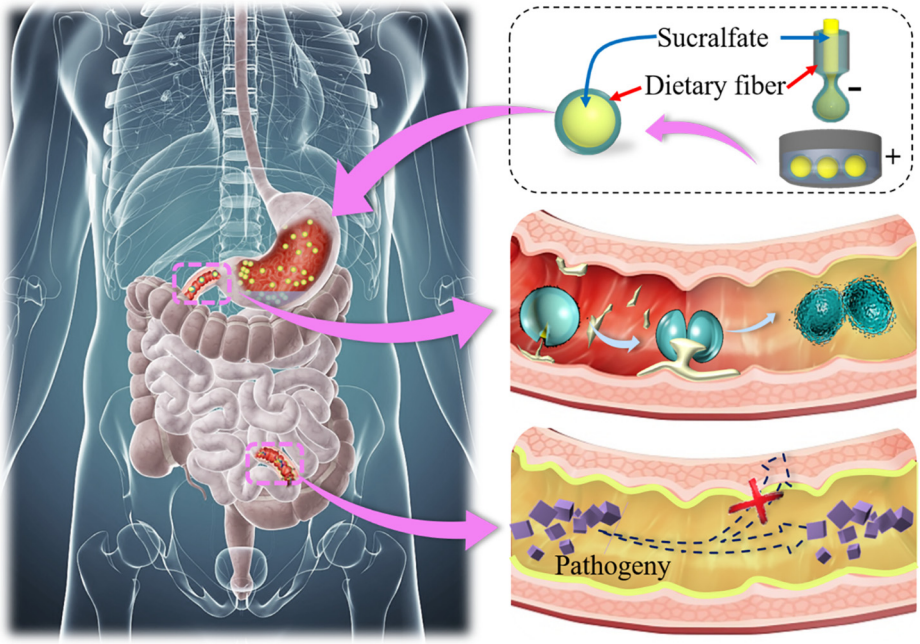

Fig. 1. (Color online) Design and fabrication of the biomimetic intestinal barrier. Schematic illustration of the fabrication and application of the microfluidic encapsulated sucralfate microcapsules that line the whole gut and perform a biomimetic intestinal barrier to protect the body from luminal pathogeny.

considerable challenges [16,33,34]. Additionally, the potential value of microcapsule encapsulated bioactive agents in building a biomimetic mechanical intestinal barrier is still unexplored.

Thus, we here employed electrostatically driven microfluidics to encapsulate viscous mucosa adhesives for constructing an unprecedented biomimetic mechanical intestinal barrier. The generated microcapsules had dietary-fibre shells that could not only protect the contents from gastric juice but also promote probiotics proliferation. After degradation in the intestine, the encapsulated inner mucosal adhesives were released and formed a consecutive physical layer on the intestine. Thus, by tuning the size and ratio of the microcapsule core-shell structure, we could modulate a controllable release of the sucralfate adhesives to form a continuous physical barrier on whole length of the intestine for simulating a mechanical barrier in the gut. Through in vitro adhesive experiment, in vivo CT imaging and IVIS study, it was demonstrated that this biomimetic intestinal barrier could effectively block the fermentation of food in the gut, reduce fat generation, decrease disease risk indexes, and prevent obesity. These results indicated that the microfluidic encapsulated sucralfate microcapsules and the resultant biomimetic intestinal barrier could provide an ideal approach for treating intestine-derived diseases.

2. Materials and methods

2.1. Materials

Sucralfate, phosphoric acid, Calcein-AM (CAM), $CaCl_2$, CMC, xanthan gum, pectin, hydroxyethyl cellulose, cellulose acetate, methylcellulose, cellulose, konjac glucomannan, dextran, corn starch, soluble starch, ethyl starch, sodium chloride (NaCl), pepsin, hydrochloric acid (HCl), pancreatin, cy5, potassium phosphate monobasic, sodium hydroxide, carbon black and alginate were obtained from Aladdin. Diodone was bought from Jinkelong Biotech Company. Porcine gut was newly bought. Normal saline was self-prepared. A high voltage power supply was gained from Gamma High Voltage Research. Transwell plates were purchased from Corning Incorporated. *Lactobacillus mansoni* was purchased from China Centre of Industrial Culture Collection. IEC-6 cells were gained from Keygene Company.

2.2. Fabrication of sucralfate

Acid-treated sucralfate was prepared before generating microcapsules. Briefly, the sucralfate was reacted with 0.3 mol/L HCl solution in water. After reaction, the gel was collected and dried. The gel was then ground into white powder. When dissolved in CMC, they formed translucent viscous liquids at first and formed gel after 12 h.

2.3. Blocking effect on molecules

A transwell system was prepared to mimic the intestinal mucosa absorption which depends on surface permeation. Glucose is the most widely distributed and the most important monosaccharide in nature. Additionally, it has a lower molecular weight than lipopolysaccharide, bacteria or other toxins. Thus, we think the blocking effect of glucose could represent the blocking effect of most pathogeny. 50 mg of materials were set on the membrane in a simulated intestinal acid. 2 mL of 10 mmol/L glucose solution was added in the filter supports and the samples were collected from the upper well after 1 h. The glucose concentration was measured using a glucose meter.

2.4. Screening of common dietary fibre

Dietary fibre was filtrated with 0.22 μm membrane before incubated with *Lactobacillus mansoni*. Before coculture experiment, dietary fibre was fabricated into gel with 2% calcium chloride ($CaCl_2$) to coculture with the probiotics. The fibre that cannot react with $CaCl_2$ was composed with alginate at a ratio of 4:1 to form a gel. *Lactobacillus mansoni* was grown in a medium without carbohydrates. After preparation, 1 mL of culture medium and gels formed by different dietary fibres were set in 24-microwell plates and placed in an anaerobic jar at 37 °C for 48 h. The wells were covered with sterile mineral oil and placed in a 37 °C anaerobic chamber for 72 h during incubation. *Lactobacillus mansoni* in a

common culture medium was set as a control. After incubation, the amount of *Lactobacillus mansoni* was calculated according to a microplate reader at 660 nm. Assays were carried out in three replicates [6].

2.5. Fabrication of the microcapsules

A microfluidic chip was fabricated for generating microcapsules. Briefly, the inner diameter of the outer capillary was approximately 300 μm, and the inner capillary had an inner diameter of 100 μm. The microfluidic device was fabricated with two coaxially assembled capillaries on a glass with transparent epoxy resin at the connection spot [16]. Sucralfate was dissolved in 2% CMC for the inner phase and 4% alginate was used as the outer phase. A voltage power supply was connected to the needle and the collecting bath. The outer phase sheathed the inner phase and separated into monodispersed droplets under the electrostatic interaction and shear force. The voltage, collection distance, outer phase flow velocity and concentration of alginate were modified to regulate the morphology of the core-shell microcapsules.

2.6. In vitro drug release

A total of 0.1 mg BSA-FITC was composed with 1 mL acid-treated sucralfate before fabricating the microcapsules. To investigate the in vitro release of the microcapsules, they were immersed in 4 mL simulated intestinal fluid (SIF) or simulated gastric fluid (SGF). SIF and SGF were prepared as the USP required. Briefly, 2 g of NaCl, 3.2 g of pepsin and 7 mL of HCl were dissolved in 1,000 mL of water for SGF. 6.8 g of potassium phosphate monobasic, 10 g of pancreatin and sodium hydroxide were dissolved in 1,000 mL of water for SIF (pH 6.8). 1 mL of SIF or SGF was retrieved and the fluorescence was determined by a microplate reader at 1, 2, 3, 4, 5, 6, 7 and 8 h. All experiments were performed for three replicates. The drug release (ω) was calculated according to the following equation. F_1 referred to the fluorescence intensity of microcapsules at different times. F_2 referred to the initial fluorescence intensity.

$$\omega = (1 - F_1/F_2) \times 100\%.$$

2.7. Biocompatibility of the microcapsule

The biocompatibility was analysed through in vitro and in vivo experiments including coculturing materials with IEC-6 and histological analysis of rat intestines. Briefly, sucralfate, empty capsules and microcapsules were cocultured with IEC-6 for 3 days. CAM staining was conducted for each group after 3 days. Cells without any interventions were set as a control. In vivo, the intestines were collected for haematoxylin and eosin (HE) staining after daily, respectively, being gavaged with 1 g of sucralfate, empty capsules, microcapsules and normal saline for 2 weeks. The histological structure of the intestines was then assessed.

2.8. Characterization of the intestine physical barrier

CT imaging and IVIS were used to visualize the biomimetic intestinal barrier on the gut surface in vivo [14]. In CT imaging, sucralfate was composed with diodone and encapsulated in microcapsules for gavage. The rats were anaesthetized and placed in micro-CT at 3 and 12 h. Data were collected and reconstructed into three-dimensional (3D) projections and analysed using CTvox. In IVIS, cy5 was encapsulated with sucralfate-CMC for intestinal imaging. After being gavaged with microcapsules for 3 and 12 h, the intestines were collected and imaged with an In Vivo Imaging System (IVIS Spectrum). Rats without interventions were used as the control group, and the images were normalized with the control group.

2.9. Animals and treatment

The 8–12 weeks old male Sprague–Dawley (SD) rats were from Jinling Hospital. The animals were treated according to the recommendations in the Guide for the Care and Use of Laboratory Animals of the National Institutes of Health. All the animal care and experimental protocols were reviewed and approved by the Animal Investigation Ethics Committee of Jinling Hospital. The obesity model was established in rats through feeding HFD (protein, 17.2%; fat, 62.5%; carbohydrates, 20.3%) continuously for 2 weeks. Mice administered a normal diet (protein, 17.3%; fat, 11.2%; carbohydrates, 71.5%) served as controls. 1 g of sucralfate, empty capsules, normal saline and the microcapsules were given by gavage daily. During this process, rat body weight was measured every two days. After 2 weeks, the rats were sacrificed. Stool, blood and inguinal fat pad were collected for analysis. Haematological analysis, including LDL, HDL, FFA and TBA, was performed using a Tosoh-G8 analyser (Tosoh Bioscience, Japan) following the manufacturer's manual.

2.10. SCFA measurement

Standard samples, including acetic acid, propionic acid, isobutyric acid, butyrate, isopentanoic acid, pentanoic acid and caproic acid, were dissolved in diethyl ether to prepare 0.05, 0.1, 1, 5, 10, 25, 50, 100 and 250 μg/mL solutions for a standard curve. 100 mg stool samples were mixed with 100 μL 15% phosphoric acid, 100 μL 50 μg/mL isocaproic acid and 400 μL diethyl ether. The mix was homogenated for 1 min and centrifuged for 10 min at 4 °C and 12,000 r/min. The supernatant was tested with GC–MS. Samples were assessed in a blinded manner [6].

2.11. Characterization

The adhesive, acid-treated sucralfate and CMC were analysed with FTIR spectrophotometer (Thermo Fisher Scientific Nicolet 6700) in the range of 4,000–400 cm^{-1}. Microcapsules were explored by a microscope (NOVEL NTB-3A, Ningbo Yongxin Optics Co., Ltd, China) and a field emission scanning electron microscope (FESEM, Ultra Plus, Zeiss). The real-time process was recorded with a digital camera (AE2000, Motic). The CAM staining of the cells was analysed with an Opera Phenix (PerkinElmer Inc., UK). In vitro adhesive experiment was tested with a section of intestine.

2.12. Statistical analysis

All values are expressed as the mean ± SD. Statistical analysis was performed using origin. Student's *t* test was used to determine the difference between two groups. $P < 0.05$ was considered significant. ANOVA was used to determine differences in weight change.

2.13. Data availability

The raw data and processed data required to reproduce these findings are available online (see the Supplementary data).

2.14. Ethics approval and consent to participate

The authors declare that all experiments on animal were conducted in accordance with the 1964 Helsinki declaration and that all procedures were carried out with the adequate understanding and written consent of the subjects. Animal experiments were performed in accordance with the Guide for the Care and Use of Laboratory Animals of the Institute for Laboratory Animal

Research, and approval to conduct the study was obtained from the Animal Investigation Ethics Committee of Jinling Hospital. The methods were carried out according to the approved guidelines. All applicable institutional and/or national guidelines for the care and use of animals were followed.

3. Results and discussion

In a typical experiment, a coaxial capillary microfluidic chip with the electrospray device was utilized to fabricate core-shell microcapsules with sucralfate encapsulation to build a biomimetic intestinal barrier (Fig. 2a). During this process, the inner sucralfate solution flowed through the inner injection channel when the outer phase was sheathed around the inner phase owing to hydrodynamic focusing (Fig. 2b). The flow was broken up into droplets under an open electric field and gelled with calcium chloride in the collection pool to solidify microcapsules. The fast gelation made sure that the inner phase was encapsulated inside the microcapsules, which can be proven by the uniform white-coloured regions in their microscopic images (Fig. 2c). The monodispersity of the microcapsules was first studied, and it showed good monodispersion no matter the inner or outer flow rates, voltage (U), collection distance (d) or concentration of alginate (C_{Alg}) (Fig. S1 online). The surface and cross-sectional morphologies of the microcapsules were observed in detail by scanning electron microscope (SEM) images (Fig. 2d–f). It could be seen that the shell has an obvious boundary with the core. The surface of the shell was rough and the surface of the core was relatively smooth. This structure also implied successful encapsulation that could protect the inner sucralfate from degradation and impart the whole microcapsule with controlled release ability [8,16].

Benefiting from the versatility of the microfluidic approach, many solutions can be introduced as phase fluids in microcapsule fabrication. To endow the microcapsule with barrier function, the materials for blocking the inner phase and protecting the outer phase in gastric acid were screened (Fig. 3a). We used a transwell system with different materials on the bottom to study the effect on blocking the permeation of nutrients (Fig. 3b). Glucose was selected to represent nutrients because it is the most widely distributed and the most important monosaccharide in nature. As shown in Fig. 3c, sucralfate achieved the highest effect (68% blocked) followed by xanthan gum (67% blocked) and hydroxyethyl cellulose (65% blocked). Although sucralfate has the best glucose blocking ability, it is not stable in water (Fig. S2 online). By dissolving the sucralfate powder in 2% carboxymethylcellulose sodium (CMC), the whole solution was stable for more than 1 h because of the high viscosity of CMC and it gelled after 12 h (Fig. S3a online). The formed gel, sucralfate and CMC were also explored by FTIR analysis (Fig. S3b online). The FTIR of the gel was similar to acid-treated sucralfate in many peaks and different from CMC, and it showed no reaction between sucralfate and CMC. We believe the gel was generated through slow water absorption. Hence, a uniform solution results in a stable encapsulation, facilitating the further release and practical applications. To identify the safety of the potential shell materials, 13 candidate materials were screened and cocultured with *Lactobacillus mansoni* probiotic in the gut. After screening, alginate, xanthan gum and pectin had the greatest ability to promote proliferation of Lactobacillus mansoni after 3 days coculture (Fig. 3d), which implied their safety [6]. Thus, alginate was chosen as the shell material to fabricate the microcapsule. However, the microbiota in intestine were not measured since they were not the focus of this study.

Because the microfluidic electrospray approach could precisely manipulate small amounts of fluids, CMC-sucralfate-alginate microcapsules with different morphology, including shell thickness and core volume, could be accurately fabricated by adjusting different parameters in the fabricating system (Fig. S4 online). The overall sizes of the microcapsules could be controlled by adjusting the flow rates of the inner and outer phases, voltage, collection distance and alginate concentration. The diameter of the microcapsules increased with increased alginate concentration, collection distance and inner and outer phase flow, and decreased when voltage increased. The shell thickness could be controlled by mediating the outer and inner phase flow and the voltage of the whole system (Fig. S5 online). Briefly, the shell thickness increased with increased outer phase flow, decreased inner phase flow, and increased voltage. As a result, by tuning the core-shell structure, the drug release ability of the microcapsules could be controlled. By incubating the microcapsules in simulated intestinal fluid (SIF) and simulated gastric fluid (SGF) (Fig. S6 online), the release ability of the inner acid-treated sucralfate could be tested. It could be seen that with the protection of alginate shell, the acid-treated sucralfate could survive gastric juice. This property then permitted the formation of a biomimetic intestinal barrier. Additionally, the decreasing shell thickness could result in an increased release of content in both of SGF and SIF, and microcapsules with thick shells and medium shells could protect their contents from releasing in SGF. However, the thick shell impeded the release of contents in

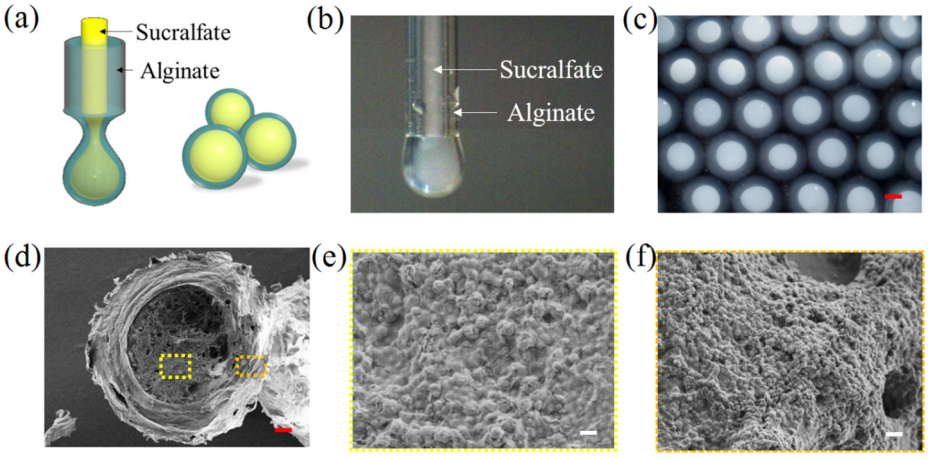

Fig. 2. (Color online) Fabrication of the microcapsule. (a) The schematic illustration of the microfluidic electrospray process. (b) A real-time image of the tip of the microfluidic device during fabrication. (c) Bright-field microscopic image of microcapsules. Scale bar is 100 μm. (d–f) SEM images of a dissected microcapsule: (d) the general structure; (e) inner surface and (f) outer surface of the microcapsule. Scale bars are 25 μm in (d), and 1 μm in (e) and (f).

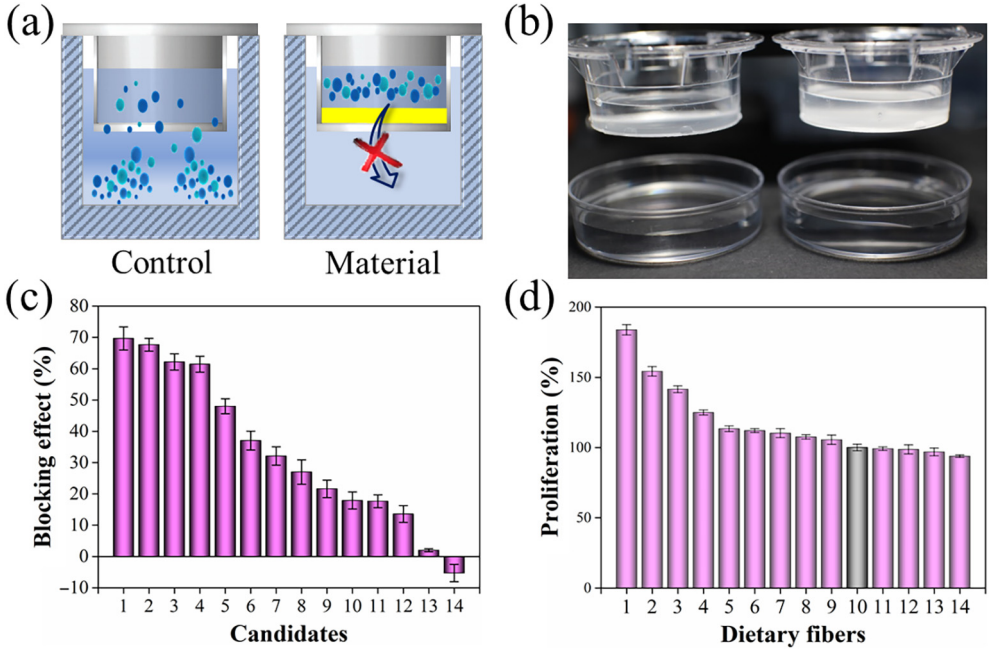

Fig. 3. (Color online) Screening of microcapsule core and shell materials. (a) Scheme of the transwell system with materials for blocking glucose. (b) The transwell system to analyse the blocking effect of materials. The left well is a control with no material on the bottom. The right well had material on the bottom used to block glucose. (c) Statistical analysis of the blocking effects of materials (candidate materials are 1. Sucralfate-CMC; 2. Sucralfate; 3. Xanthan gum; 4. Hydroxyethyl cellulose; 5. Pectin; 6. Corn starch; 7. Ethyl starch; 8. Alginate; 9. Cellulose acetate; 10. Cellulose; 11. CMC; 12. Soluble starch; 13. Dextran; 14. Konjac glucomannan). (d) The proliferation of the Lactobacillus mansoni was cocultured with different dietary fibres: 1. Alginate; 2. Xanthan gum; 3. Pectin; 4. Hydroxyethyl cellulose; 5. Cellulose acetate; 6. Methylcellulose; 7. Cellulose; 8. Konjac glucomannan; 9. Dextran; 10. Control; 11. Carboxymethylcellulose; 12. Corn starch; 13. Soluble starch; 14. Ethyl starch.

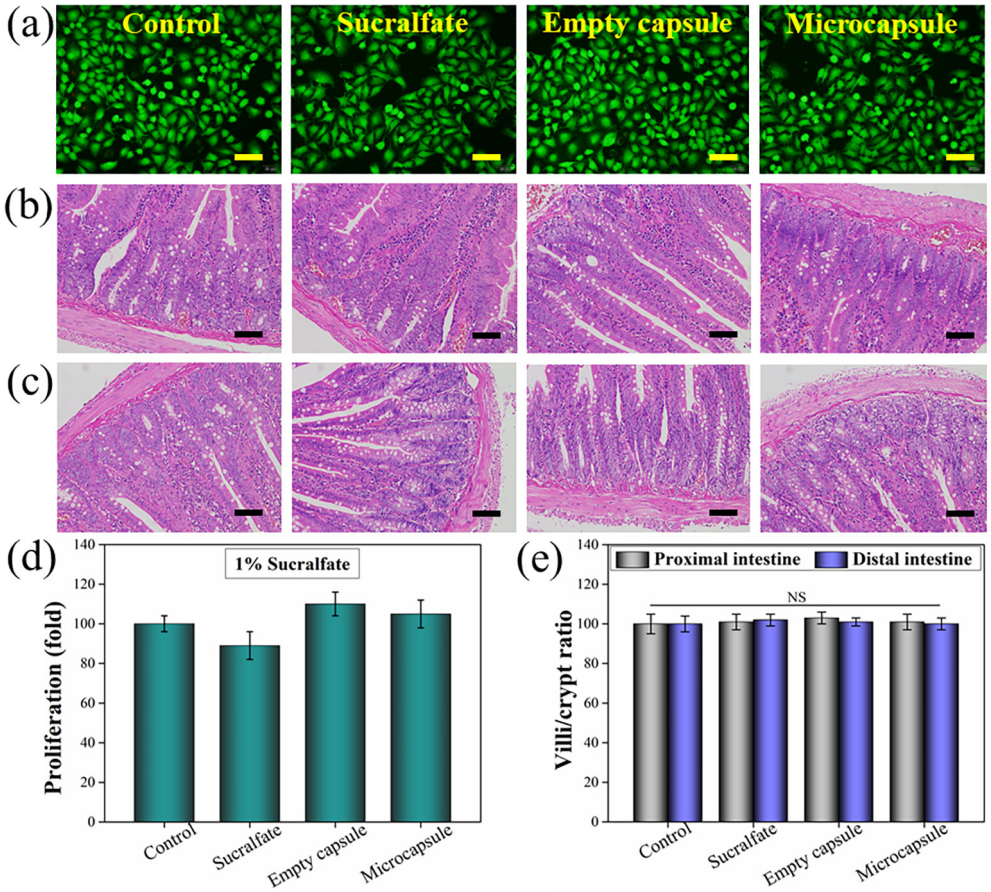

Fig. 4. (Color online) Biocompatibility of the microcapsule. (a) CAM staining and corresponding viabilities of cells after coculturing for 3 days in different groups. Scale bars are 50 μm. (b, c) HE staining of rat proximal intestines (b) and distal intestines (c) after gavage with saline, sucralfate, empty capsules and microcapsules for 7 days. Scale bars are 100 μm. (d) Proliferation of cells in control, 1% sucralfate, empty capsule and microcapsule. (e) Average villi/crypt ratio of proximal intestine (b) and distal intestine (c) in different groups.

SIF. Thus, 300 μm microcapsules with medium shells and medium cores were chosen for further experiment.

As the microcapsules were used in in-vivo experiments, their biocompatibility was examined through cytotoxicity experiments (Fig. S7 online). The results illustrated that sucralfate concentration less than 2% exhibited low toxicity to cells. Thus, we selected 1% sucralfate for further assessment. By coculturing IEC-6 cells with 1% sucralfate, empty capsules and microcapsules for 3 days, they all kept a good state in calcein-AM (CAM) staining. Among them, cells with sucralfate could survive with 10% decrease in cell numbers whereas the empty capsule and microcapsule groups showed a little increase (Fig. 4a). It could be supposed that the alginate shell could protect cells from sucralfate cytotoxicity. Additionally, the controlled release ability also contributed to lowering the cytotoxic effect of sucralfate. In vivo, the villi/crypt ratio in haematoxylin-eosin (HE) staining, which is regarded as a marker of intestinal health, was assessed. The quantification of the villi/crypt ratio showed no difference in different groups and the intestinal villus of both proximal and distal intestine stayed unchanged (Fig. 4b, c). Higher resolution images showed healthy villus, goblet cells and crypts, which exhibited uniform low pathological score according to Table S1 and Fig. S8 (online). During these experiments, no adverse effects, including diarrhoea, astriction or weight loss, were observed which suggested a good biocompatibility for this microcapsule in the digestive tract.

To investigate the potential of the sucralfate forming biomimetic barrier, an in vivo experiment was first carried out using a normal intestine model (Fig. 5a). Sucralfate-CMC was spread on the intestine and carbon black was used to mark the position of the biomimetic barrier. It could be seen that the sucralfate flowed slowly and could stick on the intestine under SIF wash, which proved that it could form a biomimetic barrier (Supplementary Movie online). In vivo CT imaging and IVIS were analysed to further demonstrate the distribution and continuity of the biomimetic intestinal barrier on the intestine. It could be demonstrated that before being gavaged with the microcapsule, there was no signal on the image (Fig. 5b, c); After being gavaged with microcapsules for 3 h, the stomach and the duodenum showed high-density and continuous signal, which indicated a disperse biomimetic intestinal barrier diffusing on the upper digestive tract. The highest density in the stomach and the end of the intestine suggested that part of the microcapsules passed the digestive tract and the others remained in the stomach. After 12 h, almost the whole intestine was covered with a thin layer continuous signal. The end of the intestine had the highest density and the previous part was covered with a relatively lower density signal. This result demonstrated that the microcapsules passed through the intestine and released their contents. The CT and IVIS images all illustrated that the microcapsules formed a stable gelling barrier on the mucosa, which contributed to blocking the invasion of luminal contents. Thus, this biomimetic barrier could block the invasion of pathogeny or even small molecules. Owing to the complex environment of intestine, there are some places in upper intestine were not covered with the gel but we think it is enough for therapy.

The formation of a biomimetic barrier could enhance intestinal function and prevent intestine-derived diseases [1,2]. Among these diseases, obesity is a global public health issue that contributes to

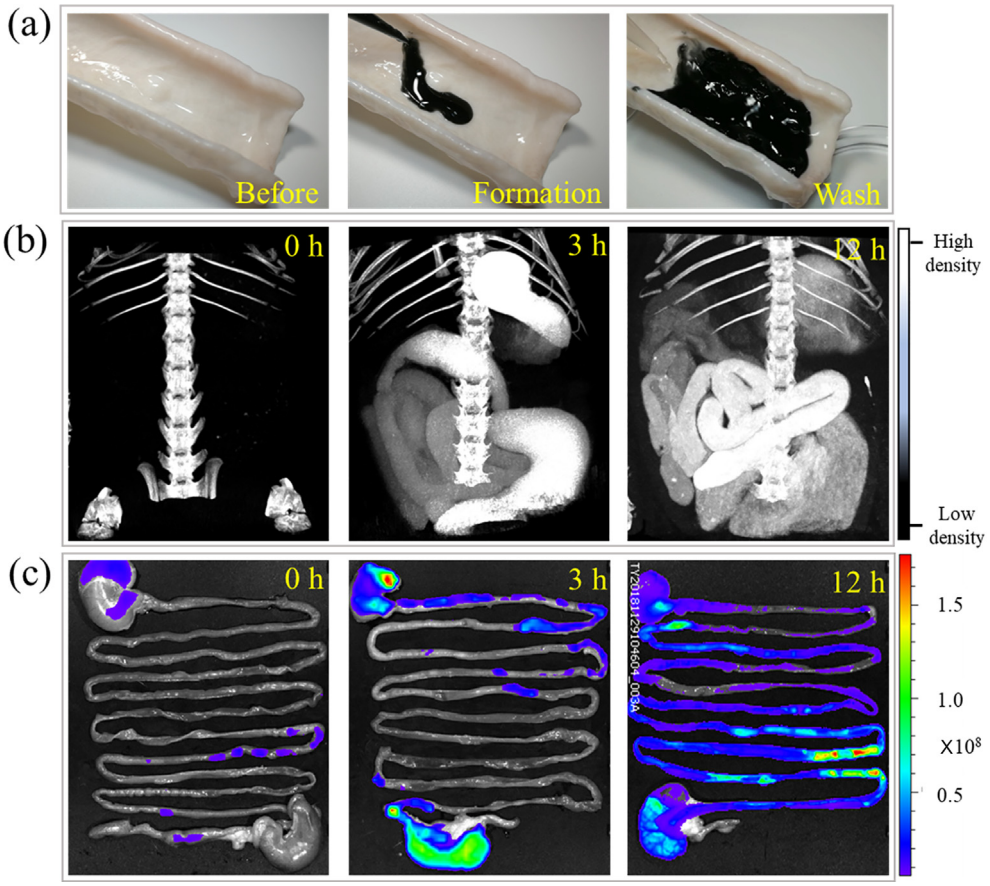

Fig. 5. (Color online) Characterization of the formation of a biomimetic intestinal barrier in vitro and in vivo. (a) In vitro adhesive experiment. (b) 3D reconstruction of CT images after gavage with microcapsule for 3 and 12 h. Rats with no intervention were set as a control. (c) IVIS images of biomimetic barrier at 3 and 12 h. Normal rat intestine was set as a control.

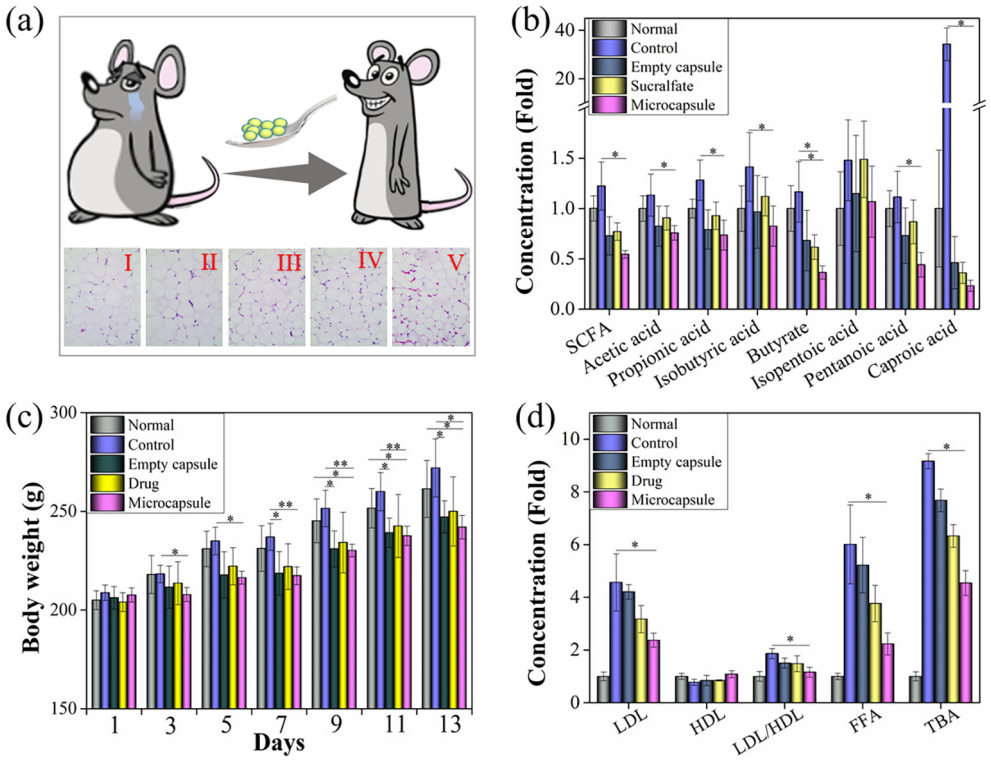

Fig. 6. (Color online) Therapeutic effect of the biomimetic barrier on preventing HFD induced obesity. (a) The schematic diagram of reducing body weight by using gavaged microcapsules. (I–V) Adipose tissue in normal, control, sucralfate, empty capsule and microcapsule groups. (b) Measurement of total amount and components of SCFAs. (c) Body weight of rats in different groups during 2 weeks. (d) Relevant markers of fat metabolism in rat blood.

cardiovascular disease, cancer, diabetes and so on. Increased intestinal permeation and a high fat diet (HFD) aggregate obesity and lead to higher risk of disease. Thus, it is crucial to construct a simple method to enhance intestinal barrier function and minimize excessive energy absorption. HFD has been proven to induce adipocyte hypertrophy in rats, which leads to higher risk of disease. Thus, HFD induced obesity was taken as an example to show the practical value of this biomimetic barrier (Fig. 6). As shown in Fig. 6a, compared with other groups, the microcapsule group inhibited adipocyte hypertrophy dramatically with great therapeutic effect. It could also be concluded that the control group had greatly accelerated body weight gain in 2 weeks, whereas groups treated with microcapsules significantly decreased their body weight (Fig. 6c). To study this in detail, short chain fatty acids (SCFAs) and fat metabolism factors in rat blood were investigated. SCFAs, the fermentation products of food, are important parts of daily energy and they also reflect the digestion of food in the gut [6]. The components of SCFAs are regarded as precursors to cholesterol, triglycerides and glucose. Acetic acid, propionic acid, isobutyric acid and butyrate are regarded as substrate of energy metabolism. Regarded as the precursor of cholesterol, the amount of acetic acid could reflect the state of cholesterol synthesizing process in body. The decrease of acetic acid in SCFAs of microcapsule group indicated the inhibition of cholesterol synthesis and the decrease of energy generation and storage. On the contrary, propionic acid could inhibit the synthesis of cholesterol. This acid has a compensatory rise in control and interventions lowered this effect. Butyrate has been considered as effective agent in mucosal nutrient, promoting triglyceride and glucose synthesis. Microcapsule group could effectively lower the level of butyrate. Isopentoic acid, pentanoic acid and caproic acid showed similar change in these groups. As shown in Fig. 6b, the biomimetic intestinal barrier group has the lowest total SCFA in all groups, indicating that it has the lowest amount of food in contact with the gut and microbiota which limited the generation of SCFA. This conclusion was also proven by blood markers. Blood free fatty acid (FFA), low density lipoprotein (LDL), high density lipoprotein (HDL) and total bile acid (TBA) are markers for fat metabolism. Higher levels of these factors indicate higher synthesis and fat storage. The higher ratio of LDL/HDL is usually combined with higher risk of cardiovascular disease. Compared with other groups, the microcapsule group reduced food fermentation and absorption, leading to less SCFAs, FFA, LDL/HDL and TBA (Fig. 6d). This result contributed to less body weight and smaller adipocytes proving a dramatic effect for the biomimetic intestinal barrier in preventing intestinal diseases.

4. Conclusion

In conclusion, a biomimetic mechanical intestinal barrier based on microfluidic encapsulated sucralfate microcapsules for preventing intestine-derived diseases has been built by using microfluidic electrospray. This mucosal adhesive system was composed of a probiotic promoting shell and blocking with a bioadhesive sucralfate core. Precise control of the microfluidic electrospray contributed to controllable size, thickness, type and spatial arrangement of the encapsulated sucralfate microcapsules. This tuneable core-shell microcapsule could not only protect the sucralfate from gastric acid but also control its release to form a continuous biomimetic intestinal barrier. From the in vitro and in vivo tests, it was found that this microcapsule forms a stable biomimetic intestinal barrier on the intestine that resists the wash of digestive fluids and blocks the invasion of luminal contents. The formation of a biomimetic intestinal barrier decreased the interaction between luminal contents and mucosa contributing to preventing HFD induced obesity. These features indicated that our biomimetic mechanical intestine barrier provides an ideal approach for preventing intestine-derived diseases.

Conflict of interest

The authors declare that they have no conflict of interest.

Acknowledgments

This work was supported by Projects of Jiangsu Social Development (BE2016752, BE2017722), Distinguished Scholars Foundation of Jiangsu Province (JCRCB2016006) and Key Project of Science Foundation of the 12th Five-Year Plan (BNJ13J002).

Author contributions

C.Z and Y.R.Y. contributed equally to this work. Y.J.Z., J.A.R., X.W.W. and C.Z. conceived the study and participated in its design. C.Z. and Y.R.Y. participated in the fabrication of the microcapsules. C.Z. finished the remaining experiments, drew all figures and wrote this manuscript. Y.R.Y. and X.X.Z. helped write the paper.

Appendix A. Supplementary data

Supplementary data to this article can be found online at https://doi.org/10.1016/j.scib.2019.07.020.

References

[1] Kurashima Y, Kiyono H. Mucosal ecological network of epithelium and immune cells for gut homeostasis and tissue healing. Annu Rev Immunol 2017;35:119–47.
[2] Duggan CP, Jaksic T. Pediatric intestinal failure. N Engl J Med 2017;377:666–75.
[3] Haber AL, Biton M, Rogel N, et al. A single-cell survey of the small intestinal epithelium. Nature 2017;551:333–9.
[4] Bolukbasi E, Khericha M, Regan JC, et al. Intestinal fork head regulates nutrient absorption and promotes longevity. Cell Rep 2017;21:641–53.
[5] Leclercq S, Mian FM, Stanisz AM, et al. Low-dose penicillin in early life induces long-term changes in murine gut microbiota, brain cytokines and behavior. Nat Commun 2017;8:15062.
[6] Schroeder BO, Birchenough GMH, Stahlman M, et al. Bifidobacteria or fiber protects against diet-induced microbiota-mediated colonic mucus deterioration. Cell Host Microbe 2018;23:27–40.
[7] Fan JX, Li ZH, Liu XH, et al. Bacteria-mediated tumor therapy utilizing photothermally-controlled tnf-alpha expression via oral administration. Nano Lett 2018;18:2373–80.
[8] Lee TY, Ku M, Kim B, et al. Microfluidic production of biodegradable microcapsules for sustained release of hydrophilic actives. Small 2017;13:1700646.
[9] Kim DJ, Park SG, Kim DH, et al. Sers-active-charged microgels for size- and charge-selective molecular analysis of complex biological samples. Small 2018;14:e1802520.
[10] Zhang H, Qu X, Chen H, et al. Fabrication of calcium phosphate-based nanocomposites incorporating DNA origami, gold nanorods, and anticancer drugs for biomedical applications. Adv Healthcare Mater 2017;6:1700664.
[11] Norman G, Dumville JC, Mohapatra DP, et al. Antibiotics and antiseptics for surgical wounds healing by secondary intention. Cochrane Database Syst Rev 2016;3:Cd011712.
[12] Norman G, Westby MJ, Rithalia AD, et al. Dressings and topical agents for treating venous leg ulcers. Cochrane Database Syst Rev 2018;6:Cd012583.
[13] Toews I, George AT, Peter JV, et al. Interventions for preventing upper gastrointestinal bleeding in people admitted to intensive care units. Cochrane Database Syst Rev 2018;6:Cd008687.
[14] Lee Y, Deelman TE, Chen K, et al. Therapeutic luminal coating of the intestine. Nat Mater 2018;17:834–42.
[15] Shang L, Cheng Y, Zhao Y. Emerging droplet microfluidics. Chem Rev 2017;117:7964–8040.
[16] Wang H, Zhao Z, Liu Y, et al. Biomimetic enzyme cascade reaction system in microfluidic electrospray microcapsules. Sci Adv 2018;4:eaat2816.
[17] Yu Y, Fu F, Shang L, et al. Bioinspired helical microfibers from microfluidics. Adv Mater 2017;29:1605765.
[18] Chen H, Ran T, Gan Y, et al. Ultrafast water harvesting and transport in hierarchical microchannels. Nat Mater 2018;17:935–42.
[19] Yang J, Wang L, Zhang W, et al. Reverse reconstruction and bioprinting of bacterial cellulose-based functional total intervertebral disc for therapeutic implantation. Small 2018;14:1702582.
[20] Liu Y, Jiang X. Why microfluidics? Merits and trends in chemical synthesis. Lab Chip 2017;17:3960–78.
[21] Wang P, Zhang L, Zheng W, et al. Thermo-triggered release of crispr-cas9 system by lipid-encapsulated gold nanoparticles for tumor therapy. Angew Chem Int Ed 2018;57:1491–6.
[22] Zhang H, Zhu Y, Qu L, et al. Gold nanorods conjugated porous silicon nanoparticles encapsulated in calcium alginate nano hydrogels using microemulsion templates. Nano Lett 2018;18:1448–53.
[23] Wu Y, Feng J, Gao H, et al. Superwettability-based interfacial chemical reactions. Adv Mater 2018;31:e1800718.
[24] Zhang P, Zhang F, Zhao C, et al. Superspreading on immersed gel surfaces for the confined synthesis of thin polymer films. Angew Chem Int Ed 2016;55:3615–9.
[25] Zhang YS, Khademhosseini A. Advances in engineering hydrogels. Science 2017;356:eaaf3627.
[26] Kong T, Stone HA, Wang L, et al. Dynamic regimes of electrified liquid filaments. Proc Natl Acad Sci USA 2018;115:6159–64.
[27] Fernandes AC, Gernaey KV, Kruhne U. Connecting worlds — a view on microfluidics for a wider application. Biotechnol Adv 2018;36:1341–66.
[28] Fu FFSL, Chen ZY, Yu YR, et al. Bioinspired living structural color hydrogels. Sci Robot 2018;3:eaar8580.
[29] Fu F, Chen Z, Zhao Z, et al. Bio-inspired self-healing structural color hydrogel. Proc Natl Acad Sci USA 2017;114:5900–5.
[30] Li Y, Yan D, Fu F, et al. Composite microparticles from microfluidics for synergistic drug delivery. Sci China Mater 2017;60:543–53.
[31] Liu Y, Huang Q, Wang J, et al. Microfluidic generation of egg-derived protein microcarriers for 3D cell culture and drug delivery. Sci Bull 2017;62:1283–90.
[32] Wang J, Zou M, Sun L, et al. Microfluidic generation of buddha beads-like microcarriers for cell culture. Sci China Mater 2017;60:857–65.
[33] Leijten J, Seo J, Yue K, et al. Spatially and temporally controlled hydrogels for tissue engineering. Mater Sci Eng R-Rep 2017;119:1–35.
[34] Miri AK, Hosseinabadi HG, Cecen B, et al. Permeability mapping of gelatin methacryloyl hydrogels. Acta Biomater 2018;77:38–47.

Cheng Zhao received his Ph.D. degree from Nanjing University in 2019. He is now a postdoctoral fellow under the supervision of Prof. Yuanjin Zhao. His current scientific interests focus on microcapsules and their applications.

Jianan Ren is the Director of Research Institute of General Surgery, Jinling Hospital, Nanjing University. He received his Ph.D. degree from Army Medical University. His current scientific interests include open abdomen, enteral and parenteral nutrition, intestinal barrier function and inflammatory bowel diseases.

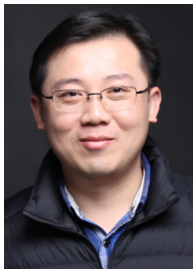

Yuanjin Zhao is a full professor at the School of Biological Science and Medical Engineering of Southeast University. He received his Ph.D. degree in 2011 from the School of Biological Science and Medical Engineering of Southeast University. In 2009–2010, he worked as a research scholar in Prof. David A. Weitz's group in Harvard University. His current scientific interests include microfluidics, ferrofluids, biomaterials, and organs-on-chips.